Gamma-ray mono-band and multi-waveband variability of blazars in the Fermi LAT era

Stefano Ciprini
University of Perugia and ASI-INAF, Italy

on behalf of the *Fermi*-LAT collaboration

Blazar variability (multi-waveband)

□ Variability found everywhere in blazars: on all time-scales in all energies (full MW variability).

□ Multi-wavelength (MW) variability: measures in the the power spectral density vs spectral energy distribution plane (PSD-SED, i.e. timescale-energy plane)

□ A possible parameter space of MW variability for blazars: third axis (L, v/c, D, m_{BH}, B, etc.)

□ Mono-band (mono-mission) studies: variability spectra, broad Power Density Spectra/Structure Functions, PDS slopes/breaks in GeV (EGRET, bias to poor statistic) and TeV blazars are found similar.

Blazar MW variability PSD-SED-plane explored
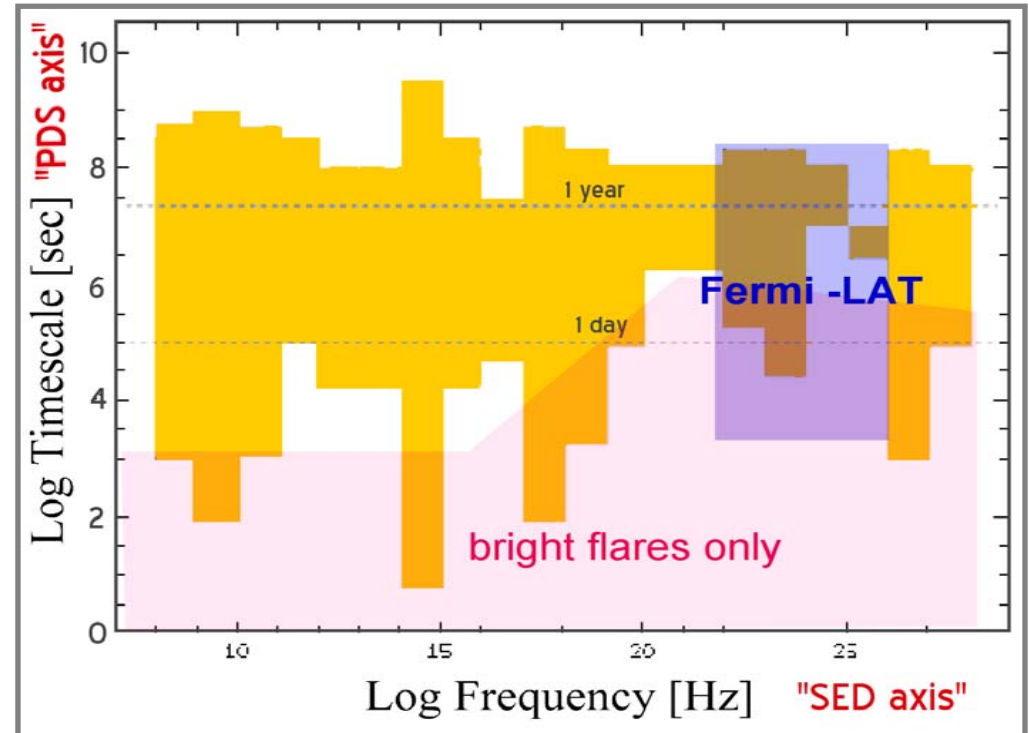
The Wagner plot

□ Broad-band MW studies: cross-correlation and time lags. MW SED modeling. Gamma-ray-synchrotro amplitude ratio studies, orphan flares, Physics of the gamma-ray emission in AGN, identification of newly discovered gamma-ray sources, spectral index hysteresis, blazar sequence and taxonomy, etc.

Blazar variability (mono-waveband)

❑ **Observed** variability (at radio, optical, X-ray bands) of blazar-like sources show the typical $1/f^a$ power spectrum decline in a wide range of frequencies f (usually a between about 1 and 3, i.e. pure flickering pink-noise, and beyond Brownian, shot-noise fluctuation modes).

❑ Warnings: Mean can vary (i.e. linear trends, fading…) and Variance is a combination of: intrinsic random scatter of errors, systematic errors, real source variability.

❑ Blazar optical variability is often characterized by great outbursts spaced out by long periods of lower emission. The distribution of flux values is similar to a Poissonian.

❑ Radio variability presents frequent peaks and long period trends. Flux values distribution is quasi-Gaussian.

❑ The LC show flares with varying amplitudes on a wide range of timescales

❑ Some high energy flares have no counterparts at longer wavelengths,

❑ Possible interband time-lags

❑ There are hints of correlation between flux and spectral variations

Stefano Ciprini
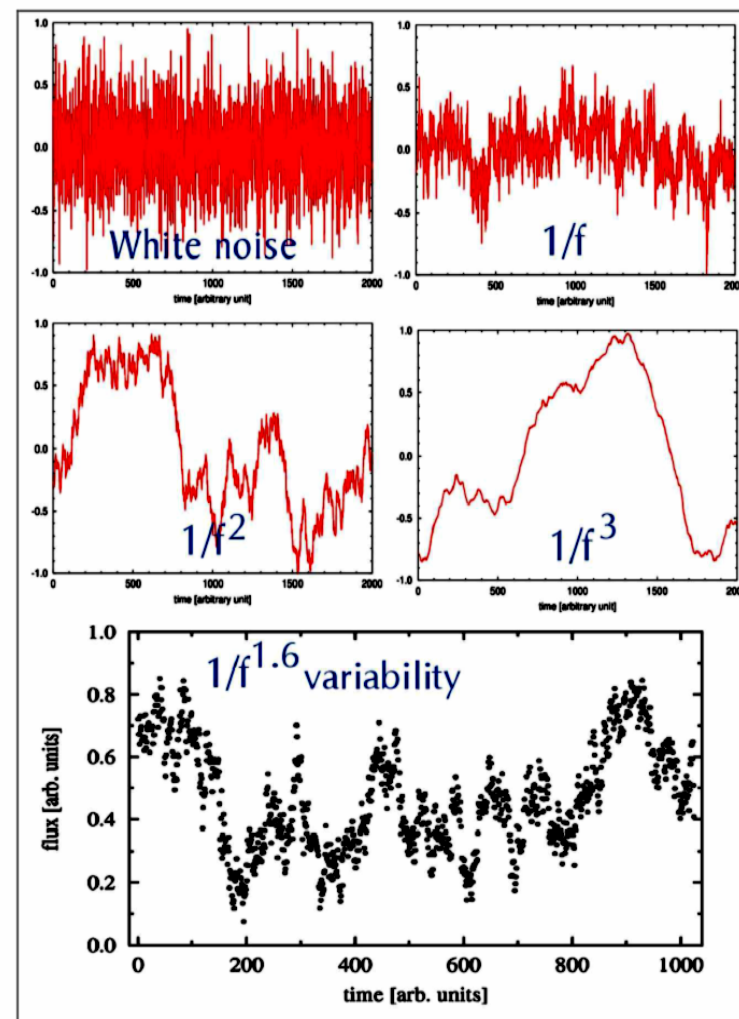
Gamma-ray variability and Fermi LAT

❑ The LAT is all-sky scanning monitor of variability and hunter for new sources and flares.

❑ The LAT has large FOV and improved sensitivity → allow variability to be investigated monitored from daily (sub-daily for most luminous flares) to month/year scales.

❑ MW follow-up can be efficiently released (Flare Advocates activity, see poster).

❑ Variability analysis of LAT detected AGN (standalone LAT data and/or MW coordinated campaigns data) is important for physical modeling (luminosity power, sizes, BH masses, Doppler factors, geometry & localization of emitting regions, MW cross correlation and lags, emission model discrimination, …).

❑ Long term monitoring yield high quality light curves for bright sources (almost evenly sampled and uninterrupted, long duration time series) which are key for break-through in AGN science

Time series and variability analysis is important not only in physical interpretation but also in:

❑ Gamma-ray Source Detection problem
(…when is a signal variable rather tha constant? → (variability indexes) -- Faint sources: real variable source or background fluctuations?

❑ Gamma-ray Source Identification problem
(variability analysis and MW cross-correlation analysis of LAT sources is an important step for a MW identification scheme)
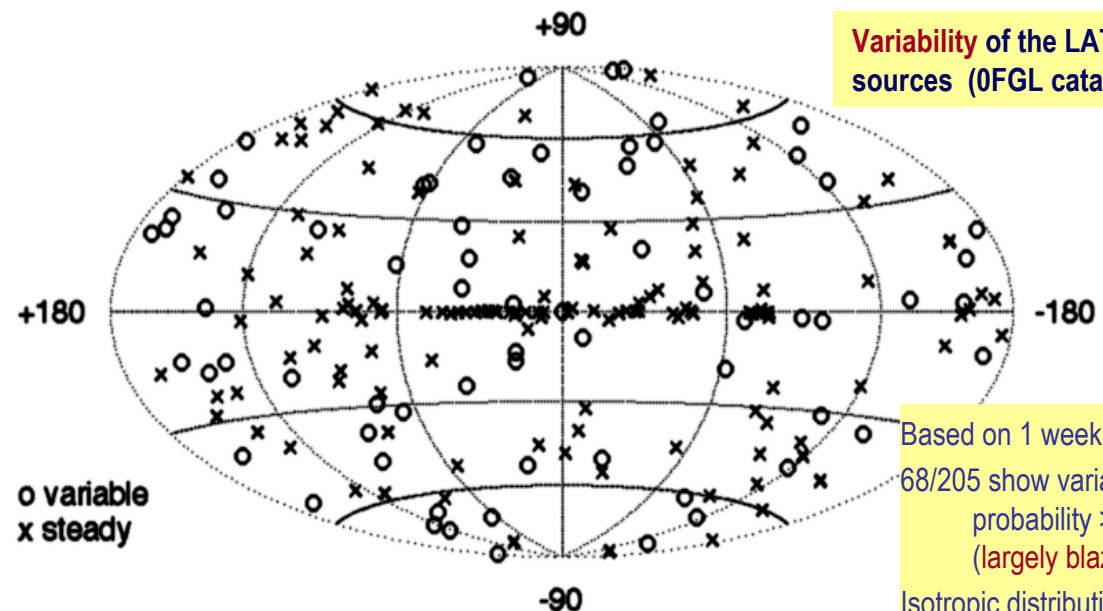
Variability of the LAT bright sources (0FGL catalog)

Based on 1 week time scales 68/205 show variability with probability > 99% (largely blazars).

Isotropic distribution ⟹ blazars

o variable
x steady

Stefano Ciprini
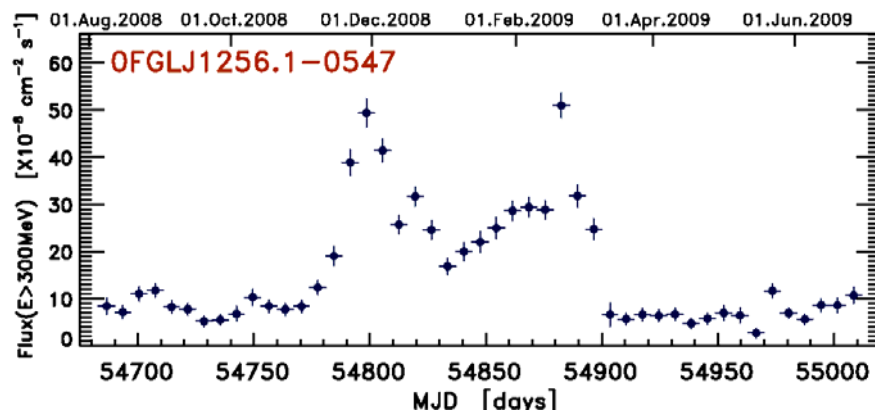
11-month weekly light curves and variabilty

**Dataset:** 3-month high confidence list of blazars (LBAS) sample (106 blazars/AGNs)
First 11 months of observations of Fermi LAT are used.
Integral fluxes above 300MeV (weekly-bin for all, + 3/4-day bin for the 15 brightest sources)

❑ For the first time a consistent and homogeneous sample of gamma-ray flux light curves
(LCs) of blazars is presented thanks to the performances and all-sky monitor of the LAT.

❑ This is a first official release of blazar light curves released by Fermi LAT.

❑ Such first look and characterization of gamma-ray blazar variability can be preparatory for
deeper and following analyses.

❑ This is a systematic study and characterization of gamma-ray blazar variability properties
(with applied methods and results limited only by the temporal resolution, weekly sampling,
and the brightness level of the LBAS sources during the first 11 months).
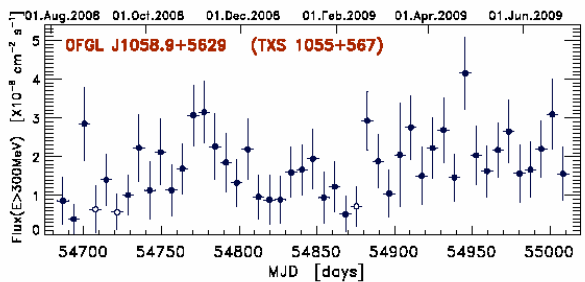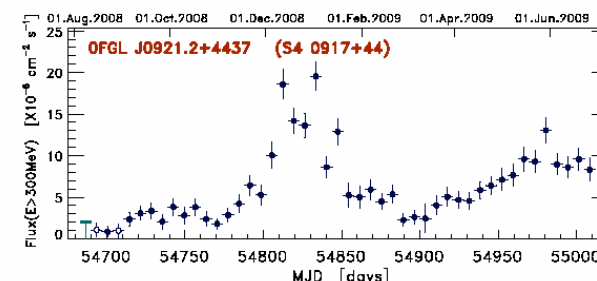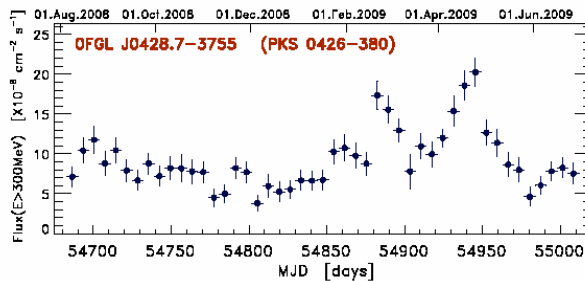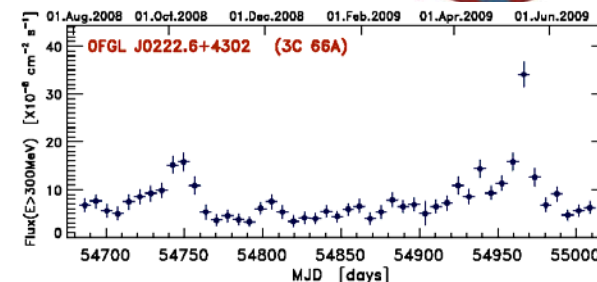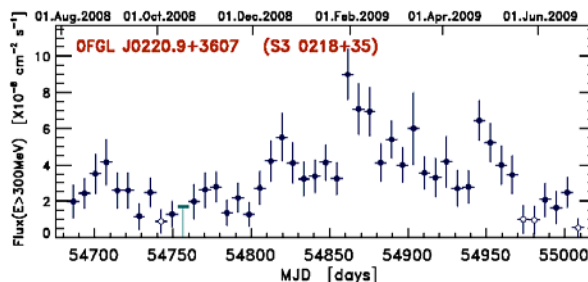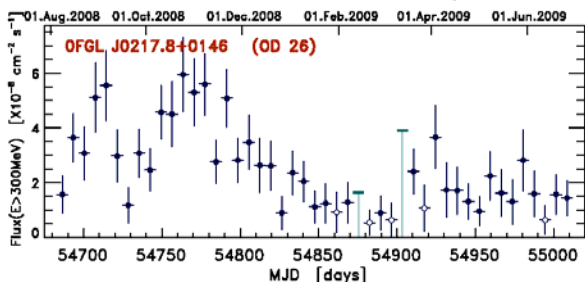

One of the "best" l.c. obtained (3C 279)
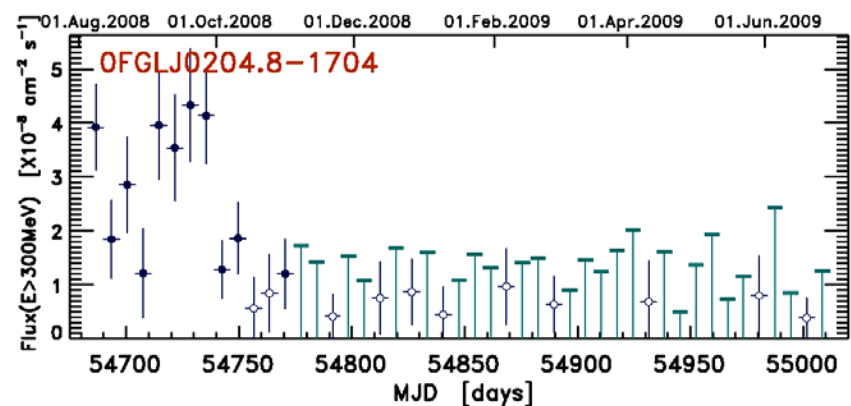
One of the "worst" l.c. obtained (PKS 0202-17)
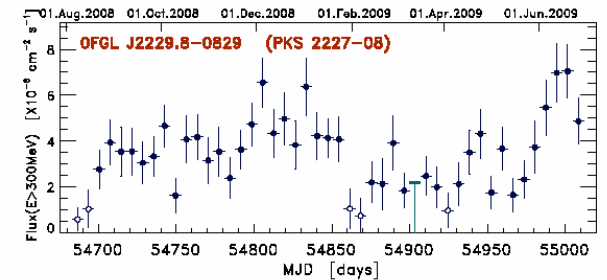
11-month, weekly, LAT light curves galore

Some examples of LAT light curves (E>300 MeV).

Some examples of LAT light curves (E>300 MeV).
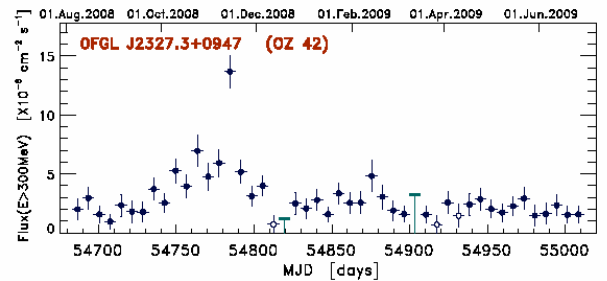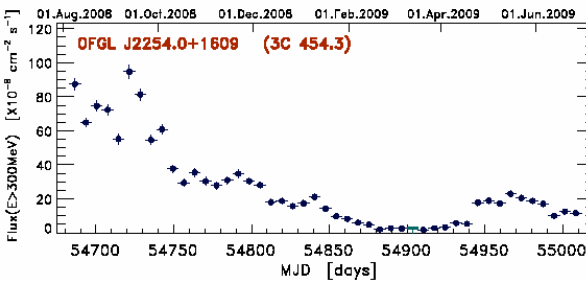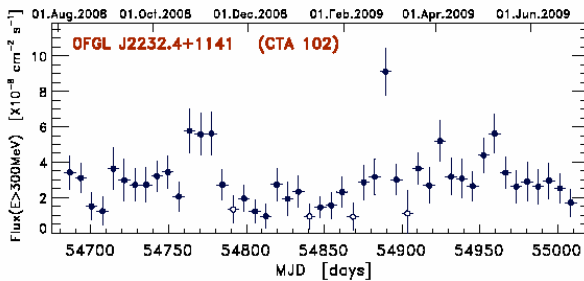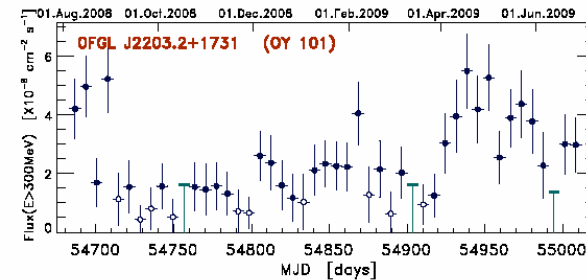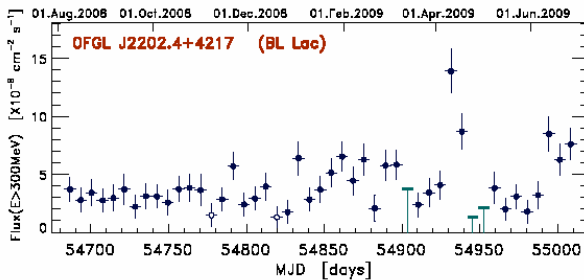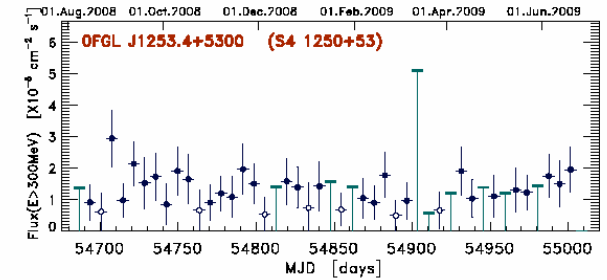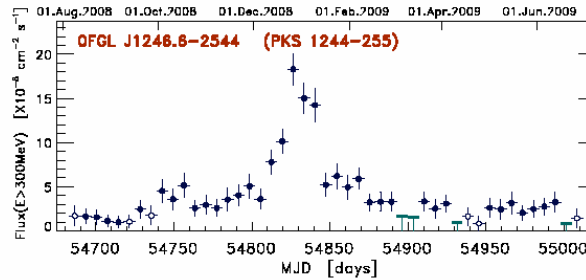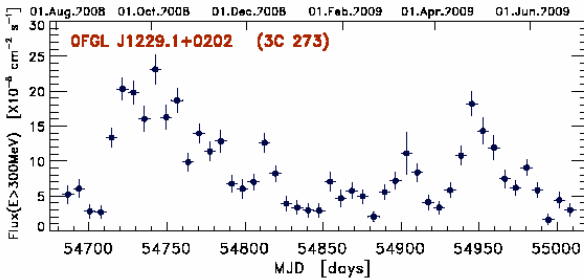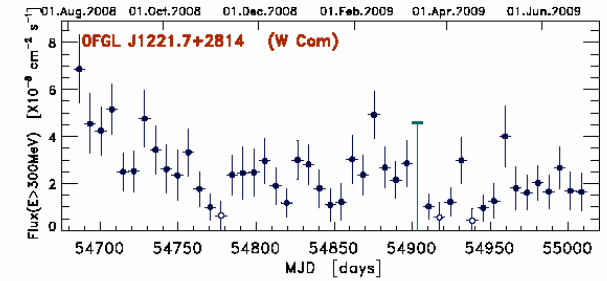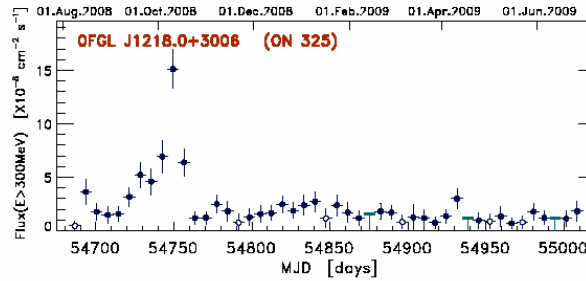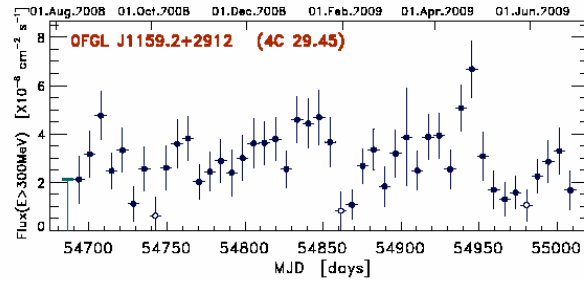
On the basis of the chi^2 test, variability was detected in 68/106 LBAS (P>99%)

$$\chi^2 = \sum_{i=1}^{N_p} \frac{(F_i - \langle F_i \rangle^2)}{(\sigma_i^2 + \sigma_{syst}^2)}$$

$$\sigma_{NXS}^2 = \frac{S^2 - \langle \sigma_{err}^2 \rangle}{\langle F_i \rangle^2}$$
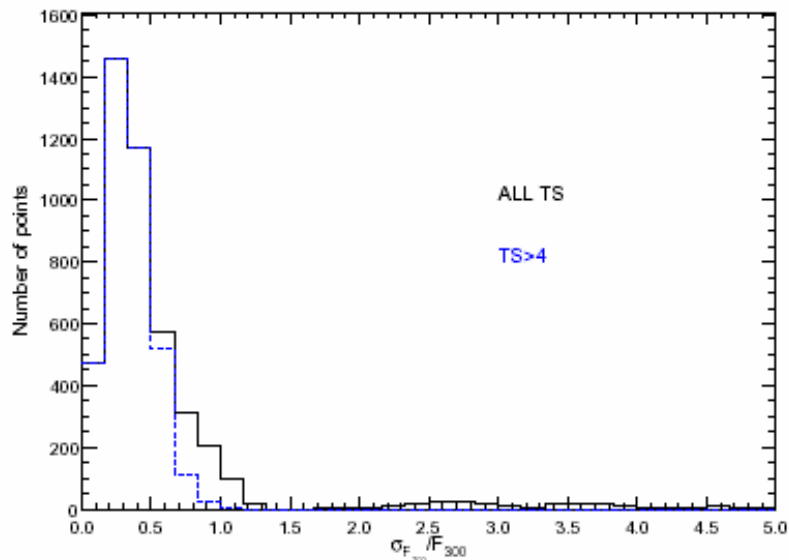
Fig. 6.— Distribution of the relative flux errors $\sigma_{F_{300}}/F_{300}$ for all the 106 LBAS light curves and all the data points. The larger values of the relative error in the distribution labeled "All TS" are due to the counting of upper limits.
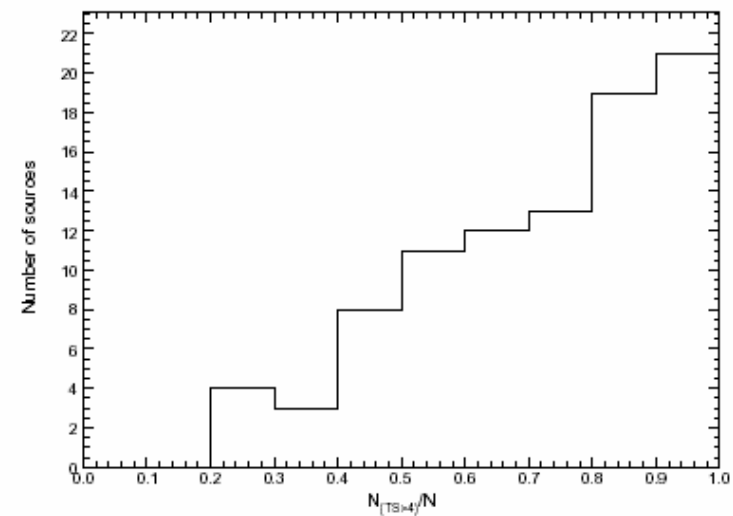
Fig. 7.— Distribution of the coverage fraction N_p/N of the observation period of each light curve.

Stefano Ciprini
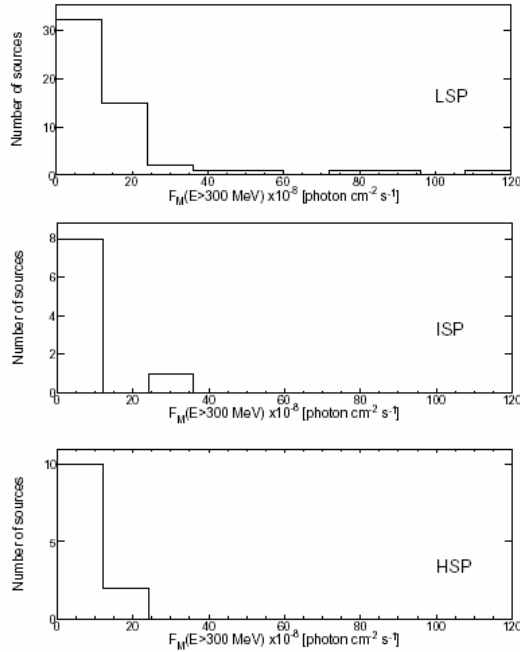
Fig. 8.— Distribution of F_M for the LSP, ISP and HSP light curves with a coverage factor $N_p/N \geq 60\%$.
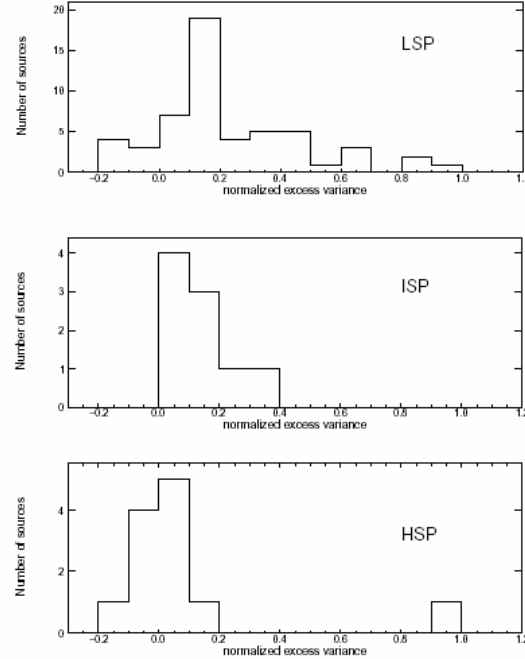
Fig. 9.— Distribution of the excess variance for the LSP, ISP and HSP light curves with a coverage factor $N_p/N \geq 60\%$.
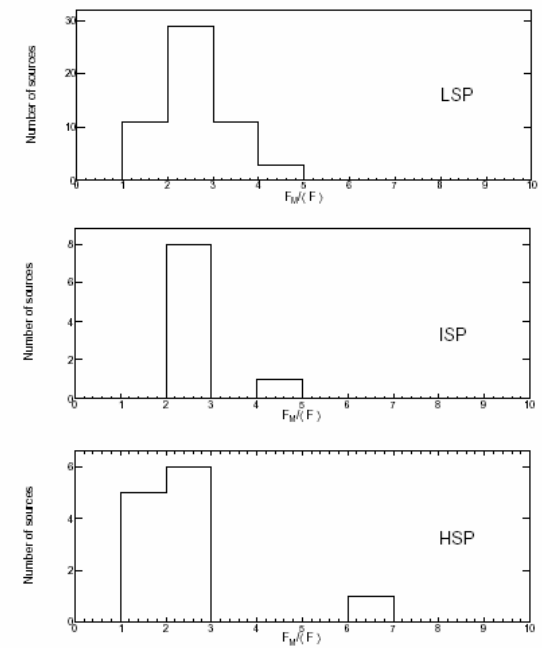
Fig. 10.— Distribution of $F_M/\langle F \rangle$ for the LSP, ISP and HSP light curves with a coverage factor $N_p/N \geq 60\%$.

84 of these sources have at least 60% of the 47 weekly bins with flux detection of TS > 4 (about 2sigma), and 56 have also a significant excess variance. High flux states do not exceed 1/4 of the total light curve range (most sources being active in periods shorter than 5% of the total light curve duration). FSRQs and LSP/ISP BL Lac objects showed largest variations, as expected. HSP BL Lac object show lower variability (with remarkable exception of ON 325), and their emission is persistent, easily detected in all the weeks.
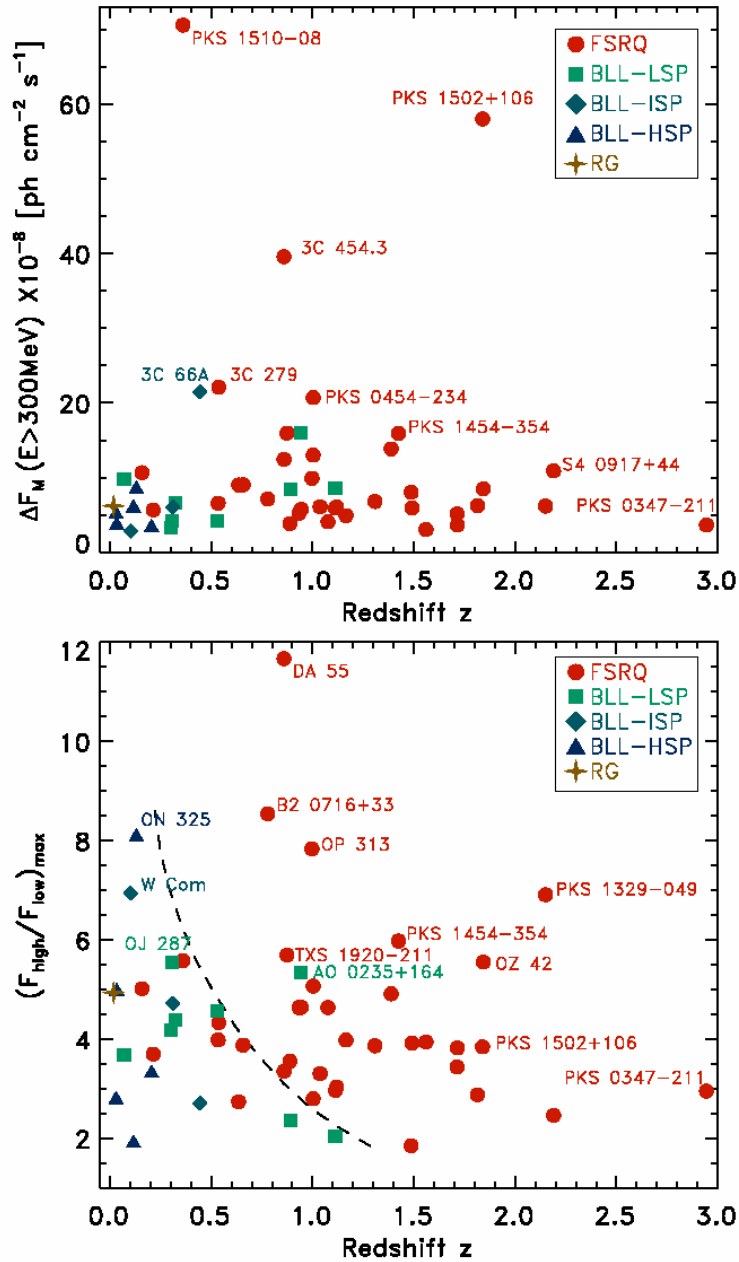
Fig. 12.— *Upper panel:* Scatter plot of the observed maximum of flux variations (F_{high}/F_{low}) in adjacent weekly bins (variations for both flux increases or decreases in subsequent weeks) versus the redshift for the 53 brightest and most variable sources of Table 1 with known z (or lower limit) and coverage $N_b/N \geq 60\%$. Most scattered sources are labeled, and different symbols and colors are used according to the classification of Table 1. *Lower panel:* Scatter plot of the maximum ratio of flux variations in adjacent weekly bins versus the redshift for the same sources. A possible separation band between BL Lac objects and FSRQs is indicated by the line.

Stefano Ciprini

Global characterization of variability (SF & DACF)

❑ 84 LBAS sources analyzed (>60% of 48 weekly bins with TS> 4 detections). Evenly sampled LCs (true UL taken into account as close to zero, and 1<TS<4 point considered with their flux-error estimations).

❑ Discrete Auto Correlation Function (DACF) and first-order Structure Function (SF) appropriate this investigation and data set. Global (not local analysis like wavelets) methods like the Power density spectra (PDS).

❑ Distribution of 1/f^a power indexes (blind application of SF with maximum lag equal to 1/3, 1/2, 2/3, 4/5 of the LC total duration).

❑ Values slightly closer to flickering, i.e. red noise, rather than a pure shot/brown-noise (peak in the 1.1-1.6 range). In agreement with some studies and PDS of optical variability samples.
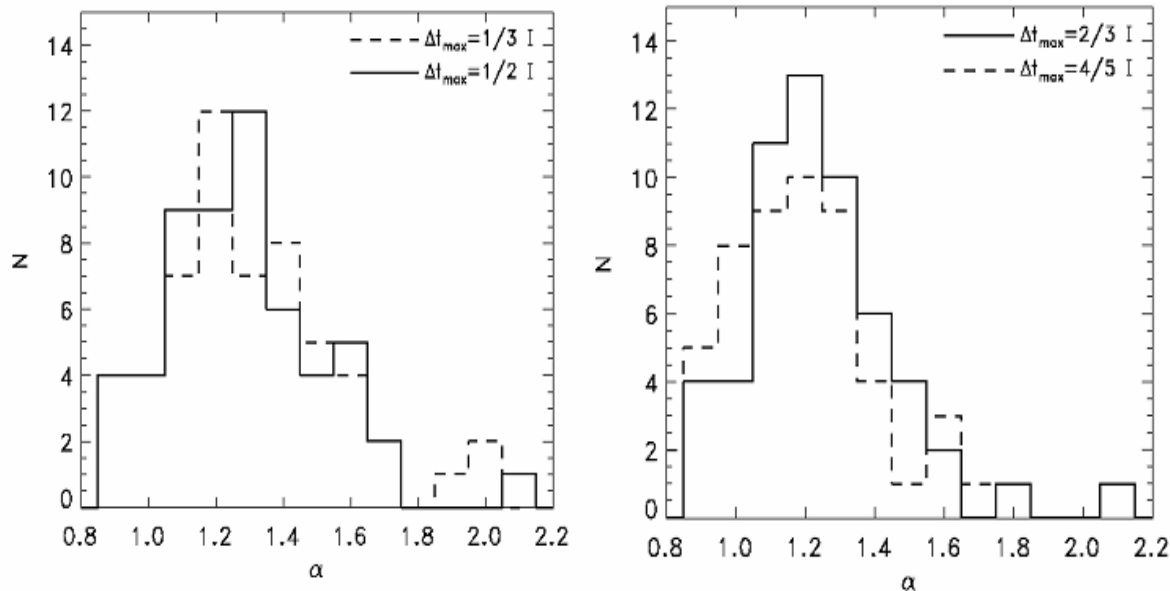
Fig. 14.— Distributions of the PDS power indexes α for the weekly light curves of the 56 most bright and variable LBAS sources, selected as explained in the text. The values are obtained applying the SF considering 4 maximum lags (1/3, 1/2, top panel, and 2/3 and 4/5 bottom panel, of the total time-range $I = t_{max} - t_{min}$). These distributions are peaked for values of the power index between 1.1 and 1.6.

Global characterization of variability (SF & DACF)

Plot with DACFs and SFs for 12 blazars, showing different autocorr. patterns, central zero lag peak amplitudes, temporal log trends/slopes, therefore different variability modes, (more flicker-dominated or shot-dominated).
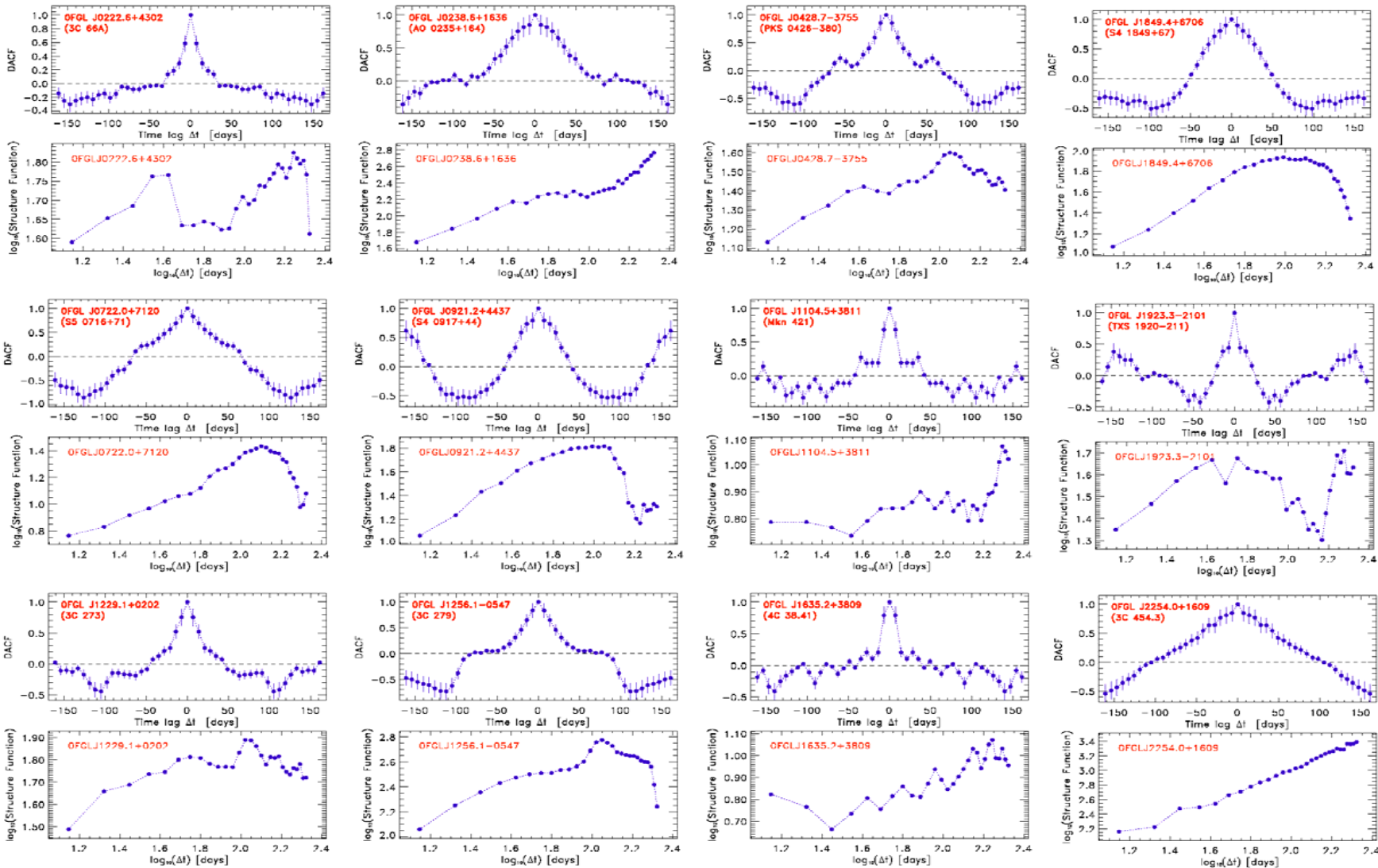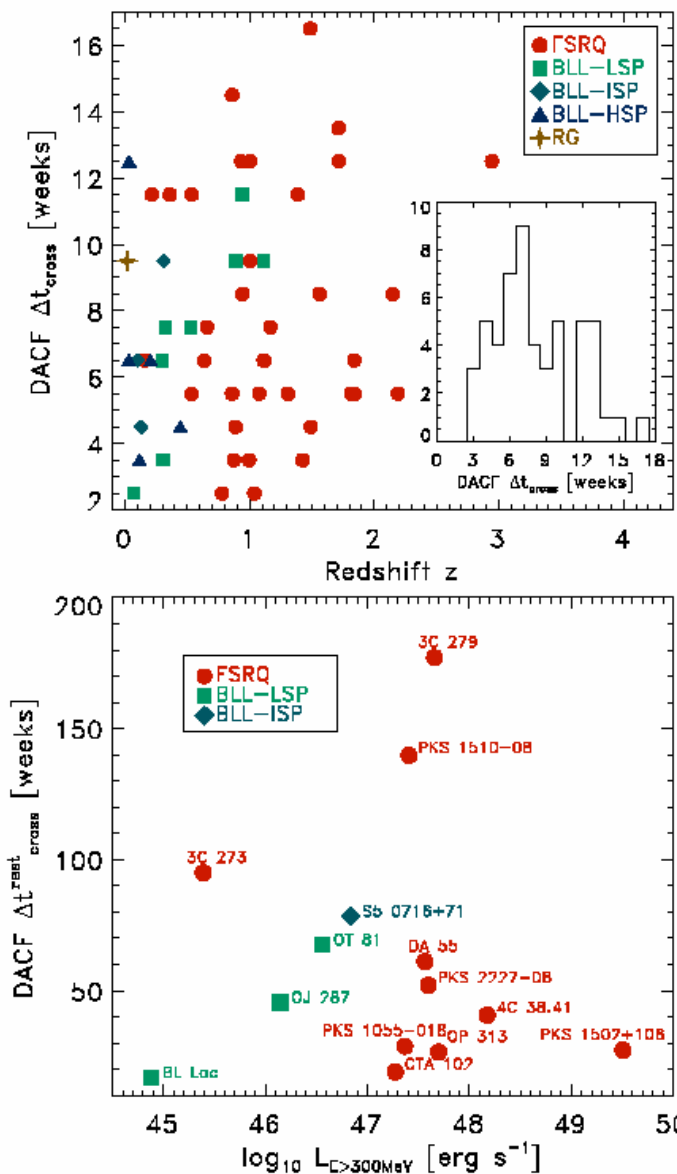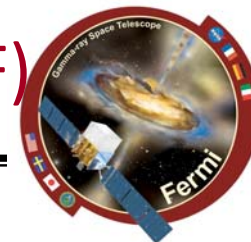
Fig. 15.— *Upper panel*: scatter plot of the DACF crossing times Δt_{cross} in weeks, versus the redshift for the 53 brightest and variable LBAS sources with known z (or lower limit). The inset panel reports the values distribution for the same set. *Lower panel*: scatter plot of the DACF crossing times in the rest frame of the source (corrected for z and beaming) versus the total apparent isotropic γ-ray luminosity ($E > 300$ MeV) in the co-moving frame, defined as in the text, for 15 of the LBAS that are also part of the MOJAVE database. 3C 454.3 is out of the plot range (with $\Delta t_{rest}^{cross} = 254.3$ weeks and $\log_{10}(L_E) = 48.1$) All sources in this panel are labeled.

Fig. 16.— Scatter plot of the PDS power index α evaluated in time domain with the SF (averaged among the SF runs performed with 4 different maximum time lags, as reported in Fig. 14) versus the observed maximum of the week-to-week flux variations. Most scattered blazars are labeled.

Stefano Ciprini

Global characterization of variability (PDS)

Systematic study of the PDS shape in the su[b]
sample of brightest blazars (28 sources) usin[g]
day and 4-day bin light curves.

Aims:

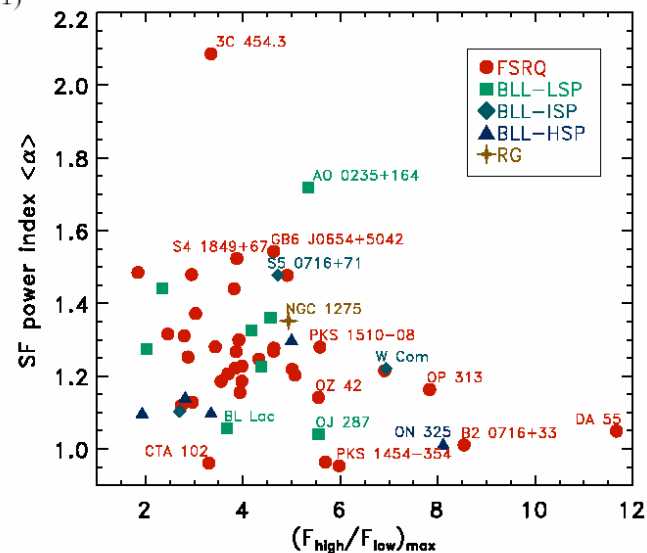   1. Search for characteristic timescales

    2. Determine power law slope (and com[pare]
to other bands)

Data used:

15 sources (9 FSRQs and 6 BL Lac's) with

3-day binned LCs

+ 13 sources (FSRQs) with 4-day binned

LCs.   No data gaps.

Analysis: PDS from Fourier transform.
Log frequency binned.   Normalized to
fractional variance.   White noise level
estimated from error bars and subtracted
  Average the PDS for FSRQs and BL Lac's.
Fit power law.

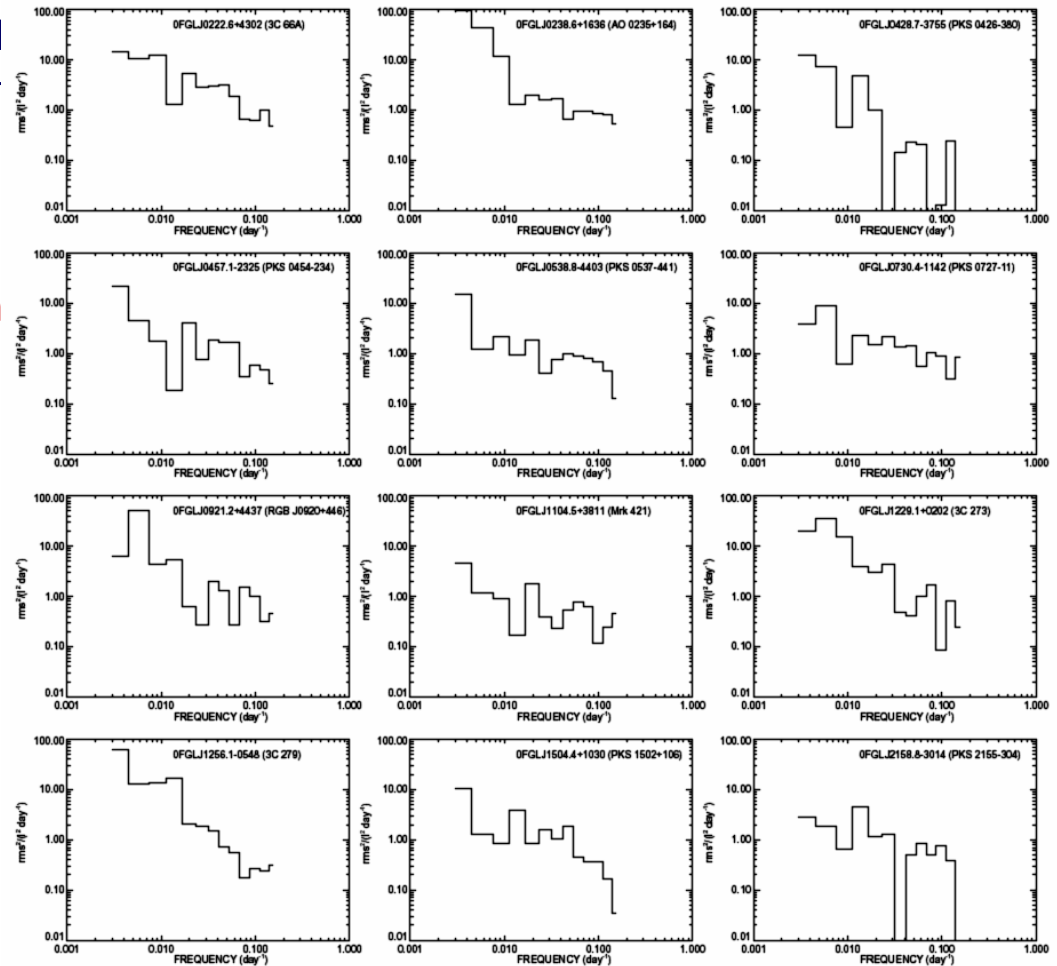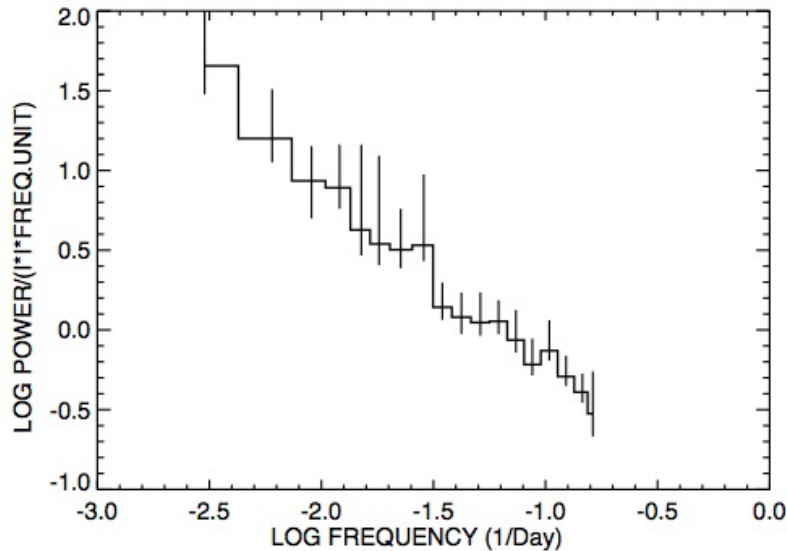Fig. 17.— Power density spectra computed from 3 day binned lightcurves for some of the brighter sources. The power density is normalized to $rms^2 \, I^{-2} \, Day^{-1}$ and the estimated white noise level has been subtracted.

Stefano Ciprini

Fig. 14

Global characterization of variability (PDS)

Average PDS for 9 brightest FSRQs

slope = -1.5 +/-0.2

and compared with the two other sets of sources

	Slope
—— 9 Brightest FSRQs	-1.5 ±0.2
······ 6 Brightest BL Lac's	-1.9 ±0.4
– – 13 Moderatly bright FSRQs	-1.6 ±0.3
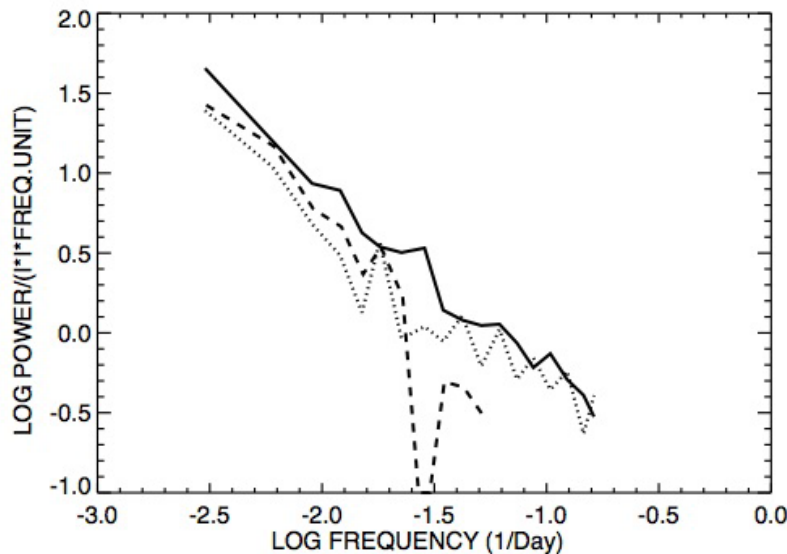
Distorted from the "true"/intrinsic shape by:

Effect	Appear as	Handled by
Statistical errors	Noise at highest frequencies	Not used in PDS fit
Analysis technique	Slight flattening (by variability >Nyquist freq)	Correction based on simulations
Systematic errors	54 Day precession period	Compare with PDS of PSRs
Stochastic variability	Noise at low frequencies	Average many sources

Stefano Ciprini

Local flare shape analysis

1. Blazars light curves of 3 days,
    except for PKS 1502+106 (weekly time bin)

2. Fit of flares with a function defined as the sum
    of the following terms:

$$F(t) = F_b + F_0 \left(e^{\frac{t_0 - t}{T_r}} + e^{\frac{t - t_0}{T_d}} \right)^{-1}$$

where T_r and T_d is rise and decay time

3. Defined two parameters which describe the flares characteristic

Flare symmetry

$$\xi = \frac{T_d + T_r}{T_d - T_r}$$

-1 < ξ < +1

So > 0 if decay slower than rise

flare length *i.e.*

$$T_{fl} = 2(T_r + T_d)$$

width at ~20% of peak flux)

Stefano Ciprini

->Flares shapes are principally
 symmetric.
->Only three flares are markedly
 asymmetric but one of this
 seems to be due to a
 sampling effect

->source shows two different
of temporal profiles:
1)   the sources with a stable
     baseline with a sporadic
     flaring activity
2) the sources with a strong
   activity with complex and
   structured features.
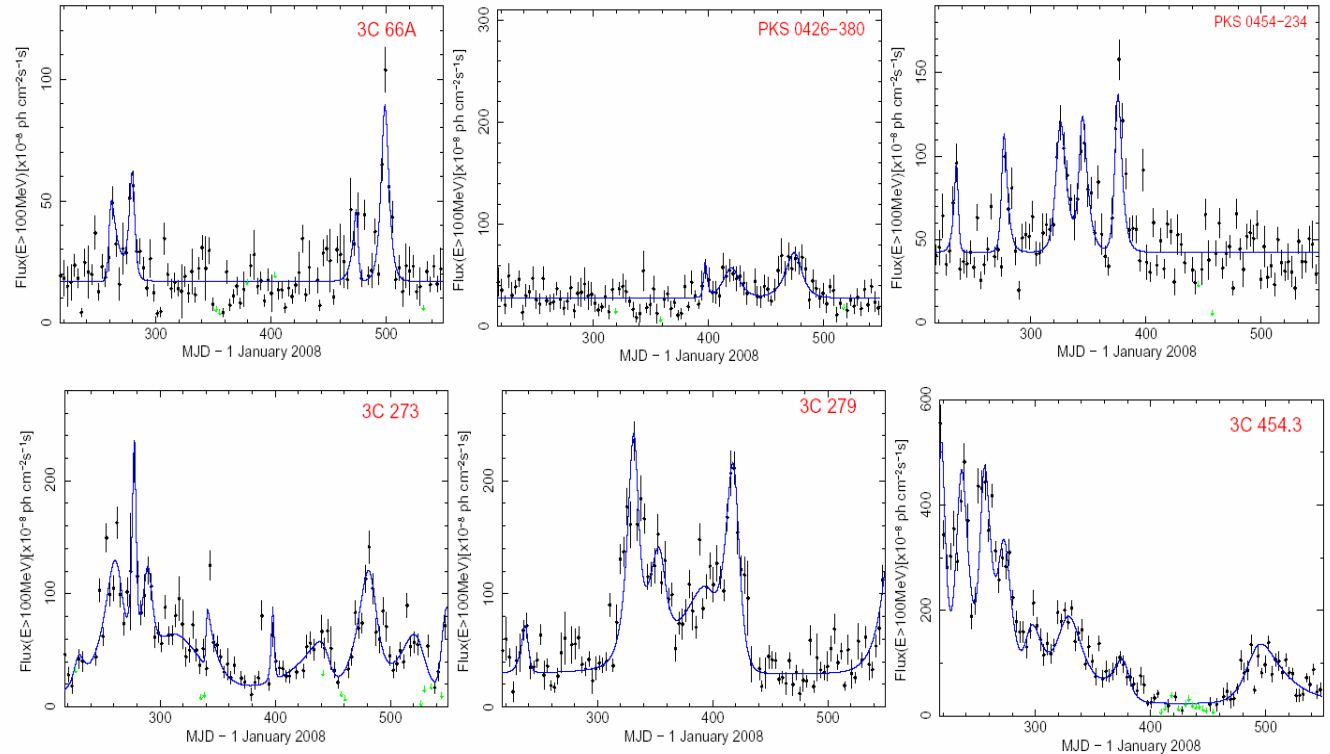
Fig. 19.— Six representative light curves ($E > 100$ MeV) of bright blazars (3C 66A, PKS 0426−380, PKS 0454−234, 3C 273, 3C 279 and 3C 454.3) obtained with 3-day bins. Data points represent detected flux values having a test statistic greater than 9, and the continuous (blue) curve represents the best fit function described in Equation 7.

Relative constancy of photon index

- slight « *harder when brighter* » effect for LPBs, IPBs
- typically, $\Delta\Gamma < 0.3$

weekly light curves

daily light curves
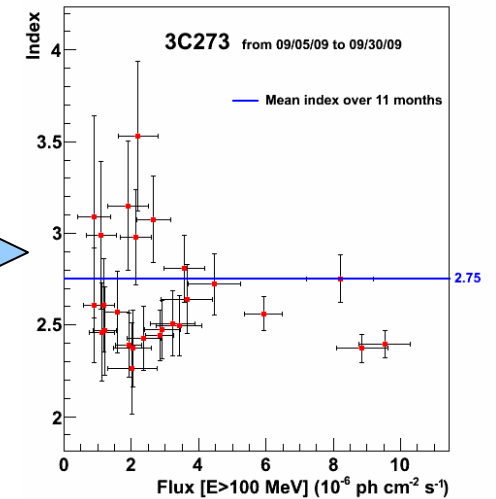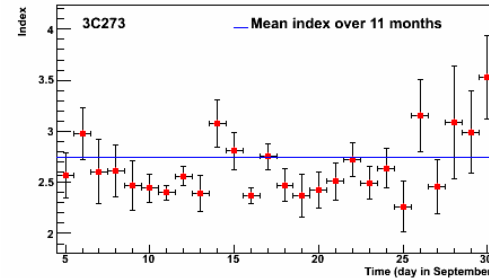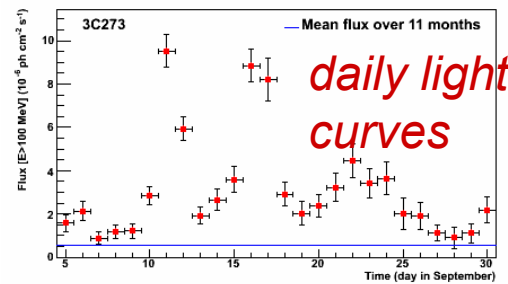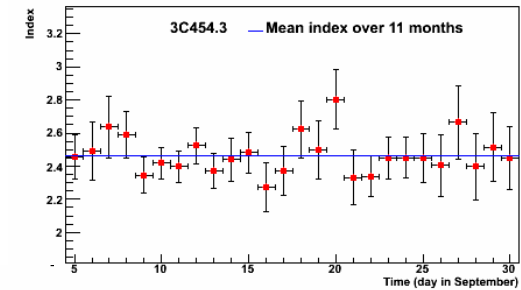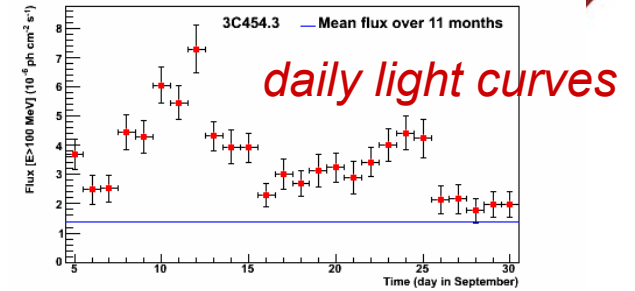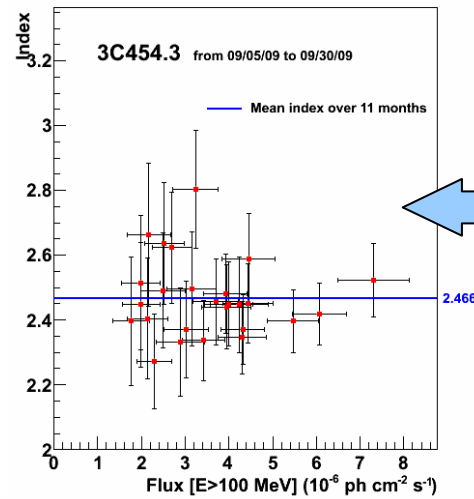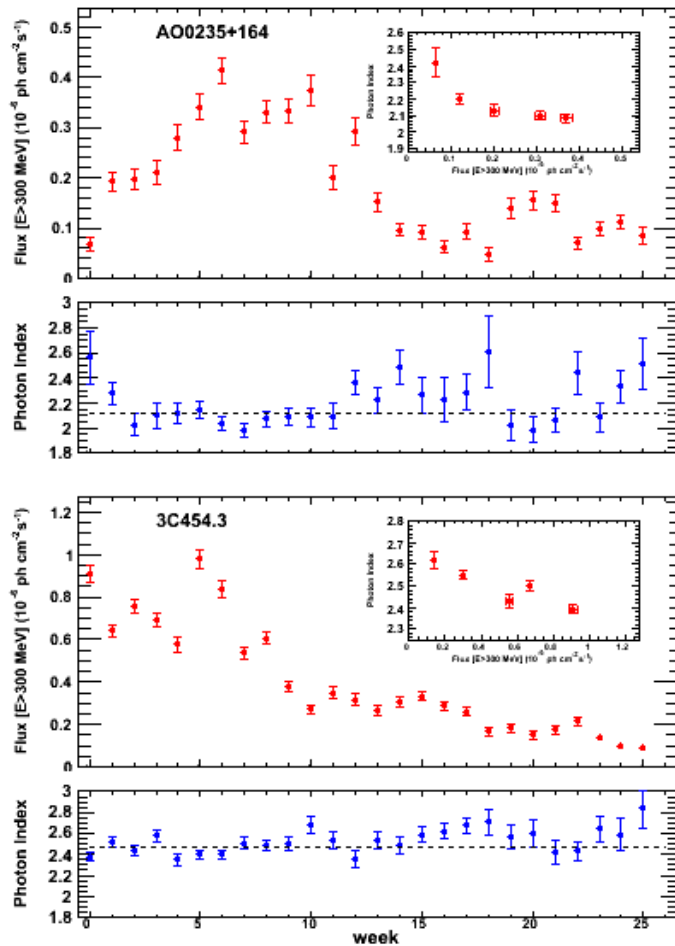
daily light curves

3C 454.3's record gamma-ray outburst
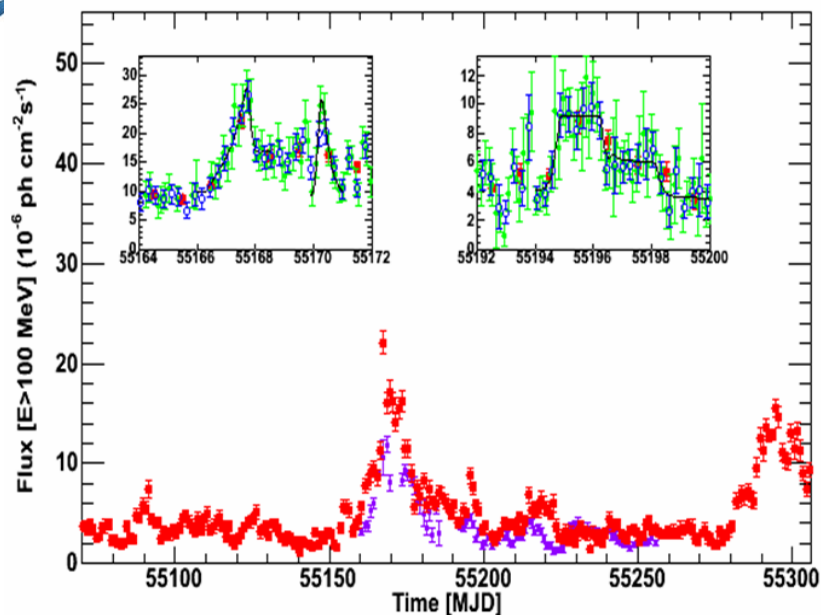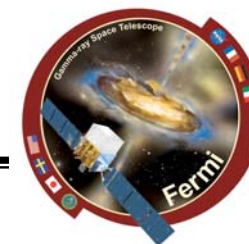
3C 454.3 light curve (0.1-200GeV band, red points). July-Aug. 2008 flare light curve shifted by 511 days, is also reported (magenta). Insets: the two periods when the largest relative flux increases took place. The red, blue and green data points are daily, 6hr and 3hr bin fluxes

Blazar 3C 454.3's Record Flare

December 2, 2009

November 3, 2009

Blazar 3C 454.3's Record Flare

November 3, 2009

Stefano Ciprini
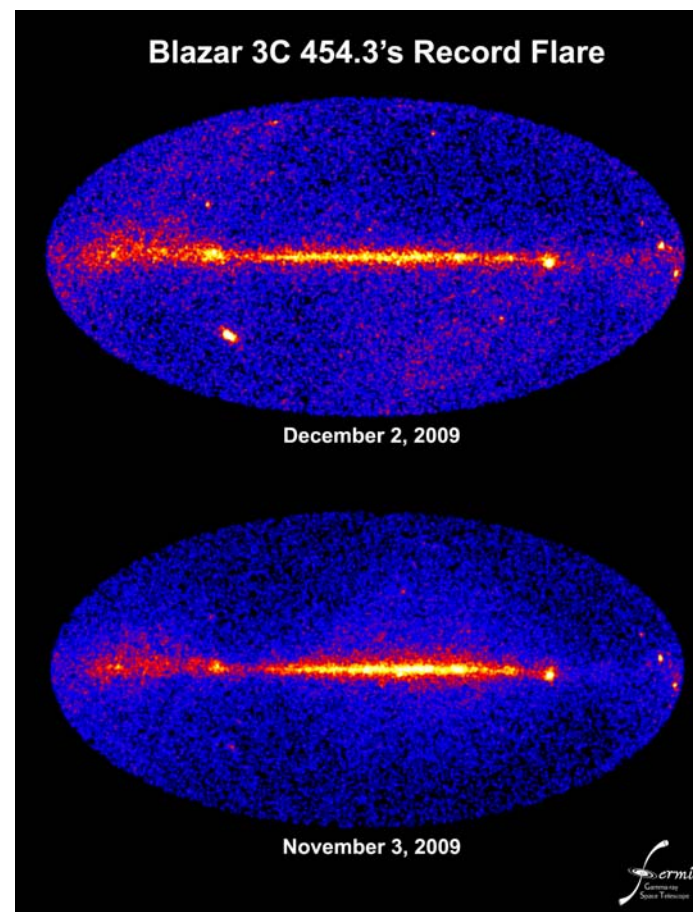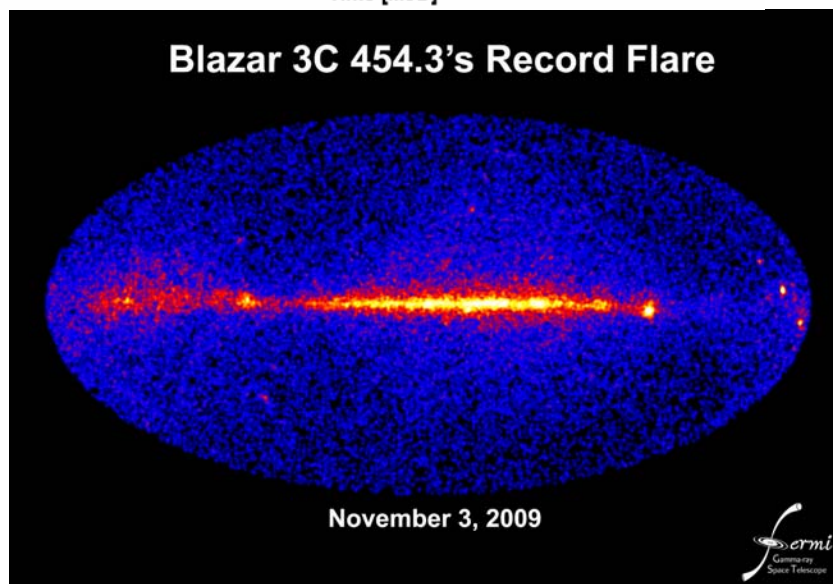
Multi-frequency variability with Fermi LAT
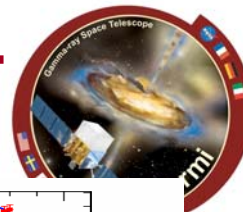
- Gamma-ray sources are inherently multi-wavelength objects (i.e. pulsars, blazars, GRBs, etc.). We want to study the multifrequency behaviour of high energy cosmic sources.

- Multi-wavelength studies are critical to maximizing the scientific return from gamma-ray telescopes in particular.

- Fermi LAT results are often optimized by coordinated simultaneous multi-frequency observations and analysis, and LAT collaboration welcomes cooperative efforts from observers at all wavelengths.

Multifrequency observations are fundamental:
- in space (sky plane): mapping, imaging, morphology, geography, identification
- in time: light curves of observed quantities, temporal physical evolution
- in energy: spectroscopy shed light on physical origin and mechanisms
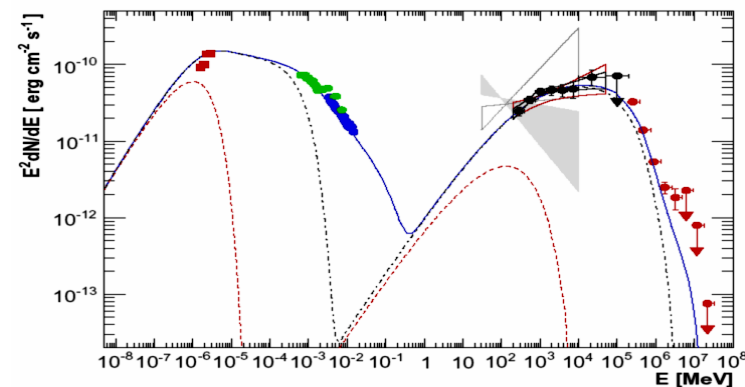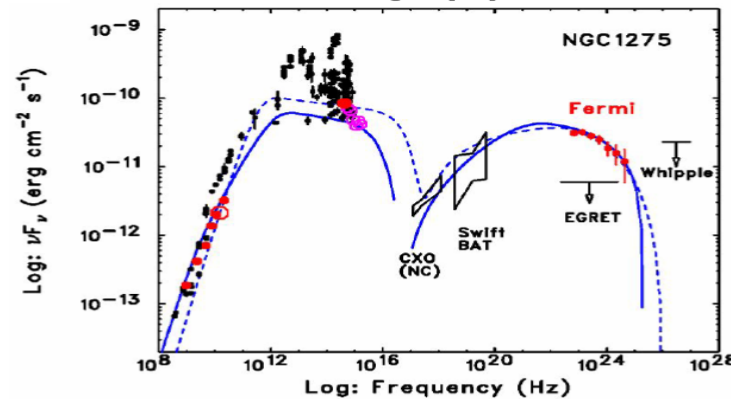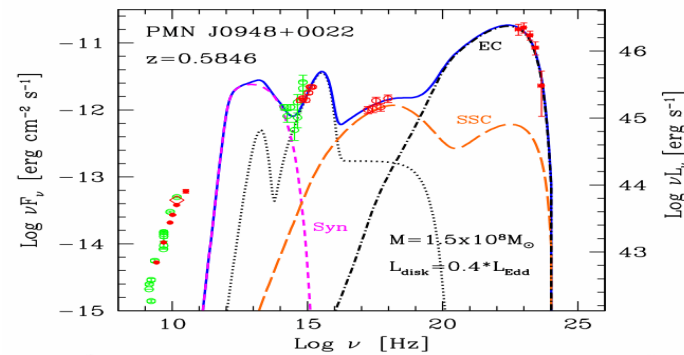
An example of the MW data thanks to Fermi campaigns.

Stefano Ciprini

An example of Fermi & MW variability: the campaign on PKS 1502+106

PKS 1502+106

Fermi - Swift 2008 multifrequency campaign:

Swift
Fermi GST

Owens Valley Radio Obs. (OVRO) 40m (USA)
Effelsberg 100m (Germany)
Metsähovi 14m (Finland)
RATAN-600 (Russia)

VLBA (Mojave program) (USA)

Kanata Telescope Higashi-Hiroshima Obs. (Japan)

Archival unpublished observations:

Spitzer
XMM-Newton
Integral
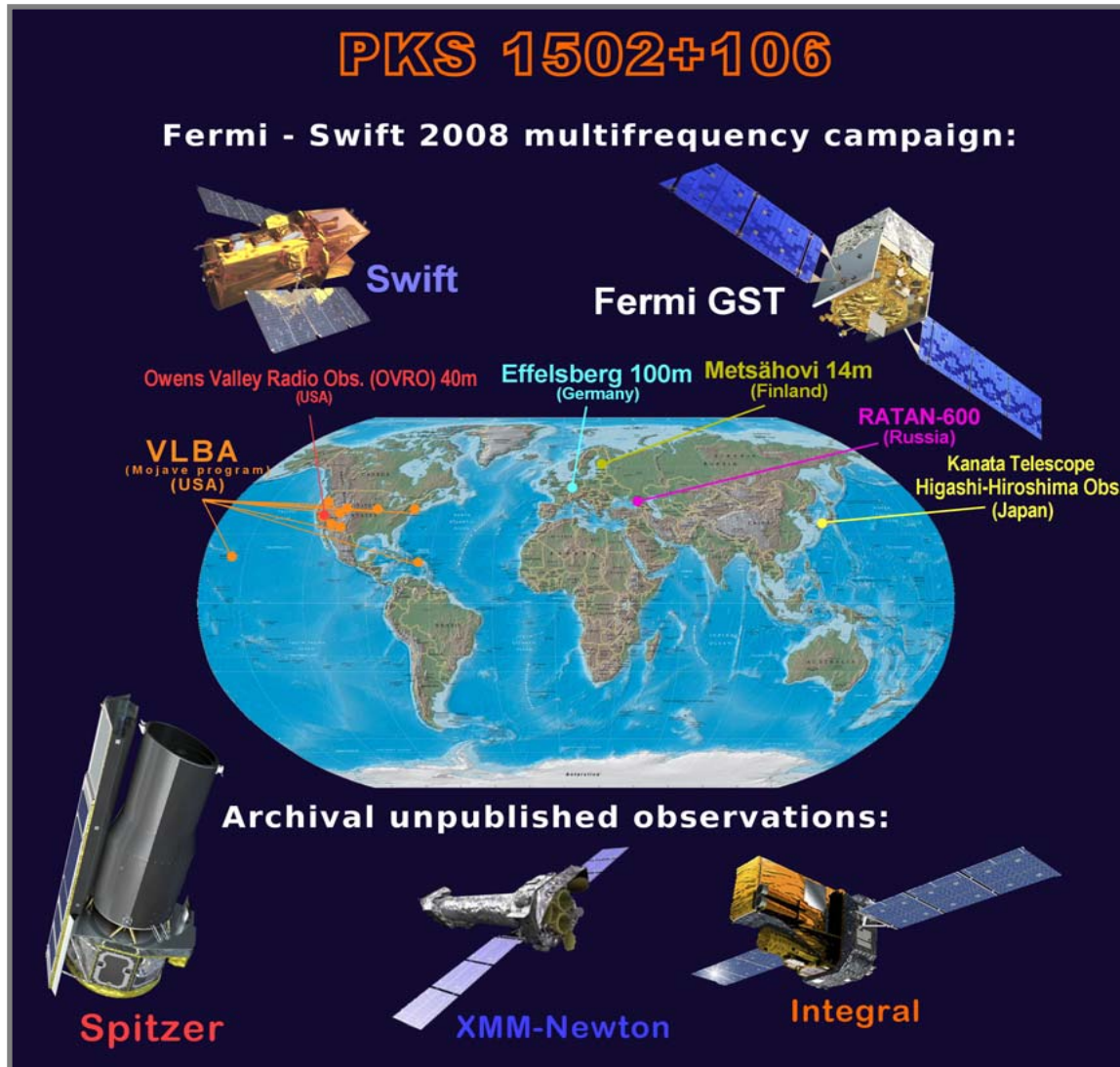
❑ A pictorial view of the facilities participating in the multi-wavelenght and simultaneous *Fermi-Swift* campaign on PKS 1502+106 (with also several radio-optical telescopes from the ground), and the other space observatories where we have took and analyzed data from their archival and unpublished (serendipitous) obs.

❑ MW analysis
- **simultaneous** (MW coordinated campaigns),
- **forward in time** (= post outburst MW monitoring),
- **back in time** (= archival mission databases) too.

Stefano Ciprini

Gamma-ray outburst of PKS 1502+106

❑ A non-PIC (not planned in advance) but ToO Campaign based on a LAT flare and the Flare Advocate activity. ATel sent, ToO to Swift performed (PI discretionary time), and a MW campaign started.

❑ Observatories involved: Swift (a 16-day monitoring), VLBA (through the MOJAVE program, USA), Owens Valley Radio Observatory 40m (USA), Effelsberg-100m (Germany), Metsähovi-14m (Finland), RATAN-600 (Russia), Kanata Higashi-Hiroshima (Japan).

❑ Archival unpublished observation analyzed too (INTEGRAL, Spitzer, XMM-Newton).
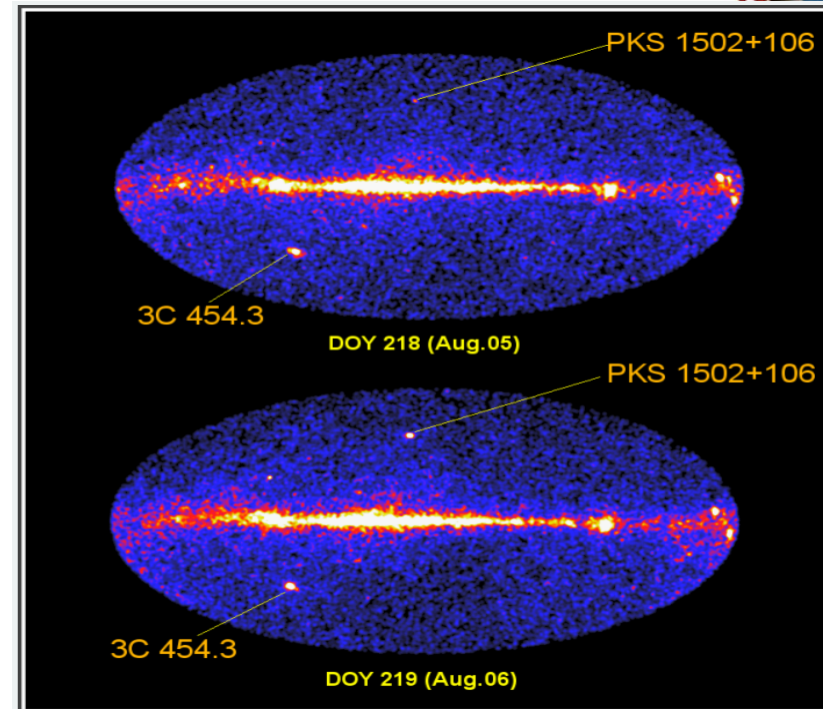
The variable daily Fermi LAT sky

4-month daily gamma-ray l.c. of PKS 1502+106
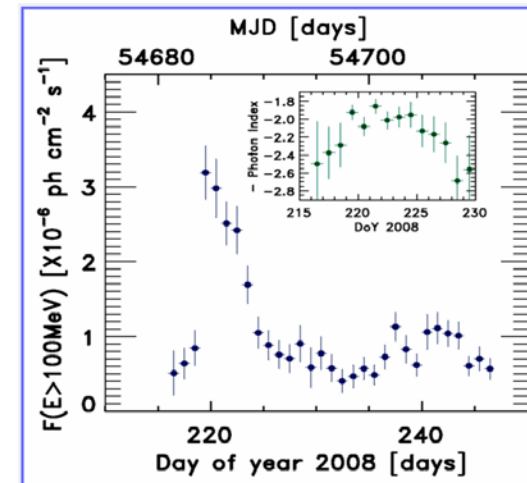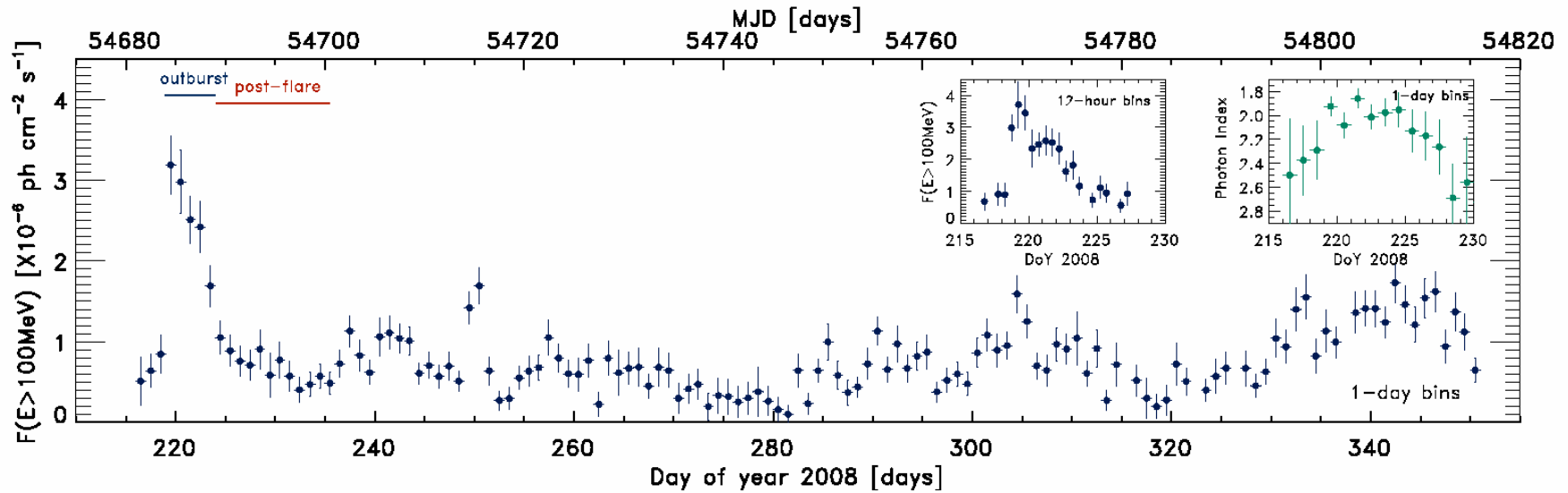
A bright source. Daily bin flux light curve during the first 4-months of Fermi all-sky survey. Cross-correlated gamma-ray and optical-UV-X-ray (Swift) variability allowed identification of this new gamma-ray blazar discovered by Fermi.

Stefano Ciprini

Multi-frequency campaign on PKS 1502+106
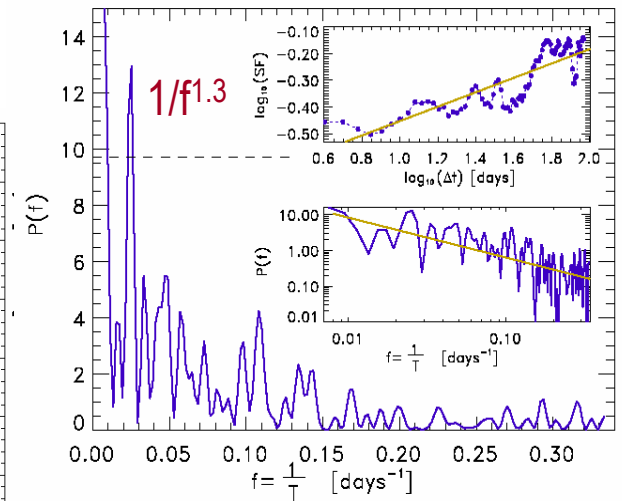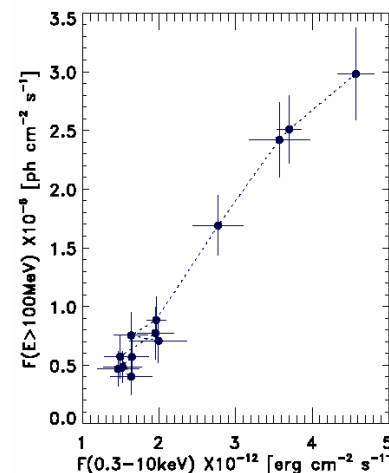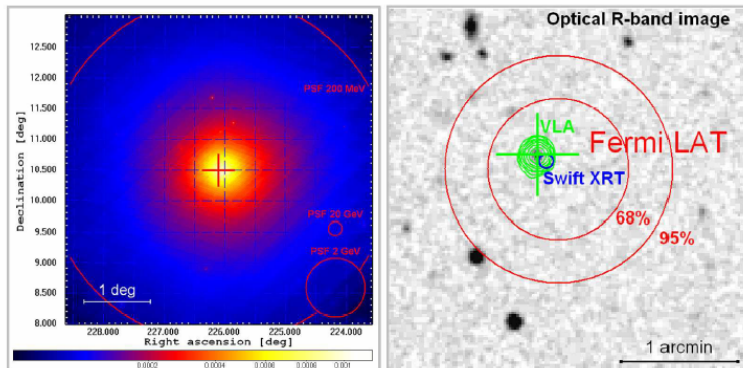
Again a MW data galore, from the coordinated simultaneous campaign and archival unpublished data.
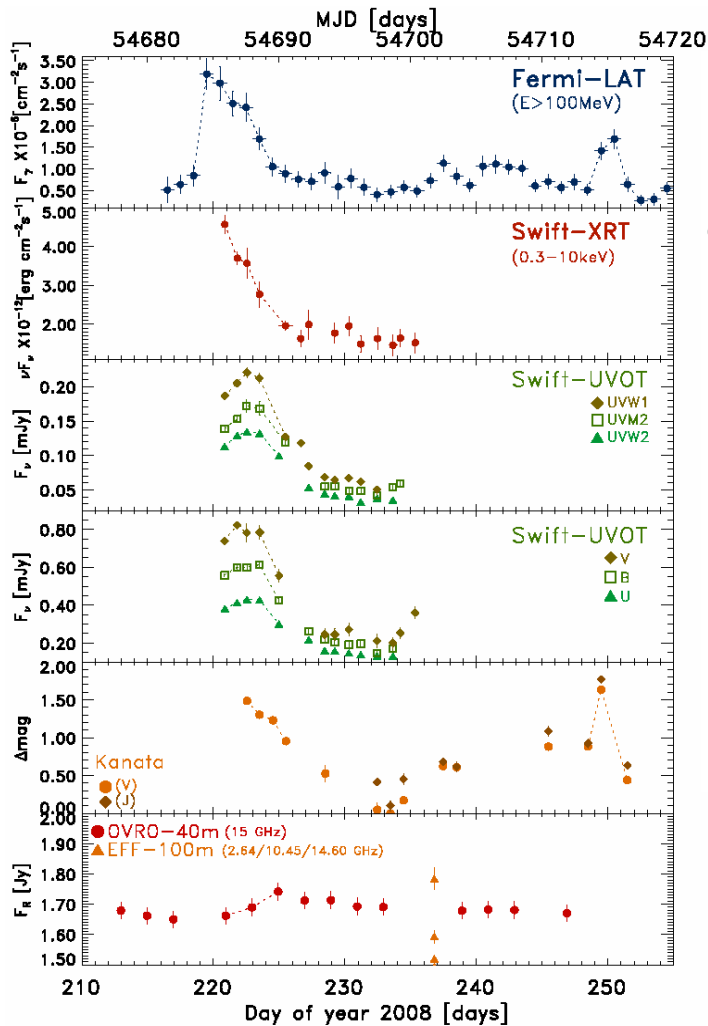
Variable multifrequency light curves
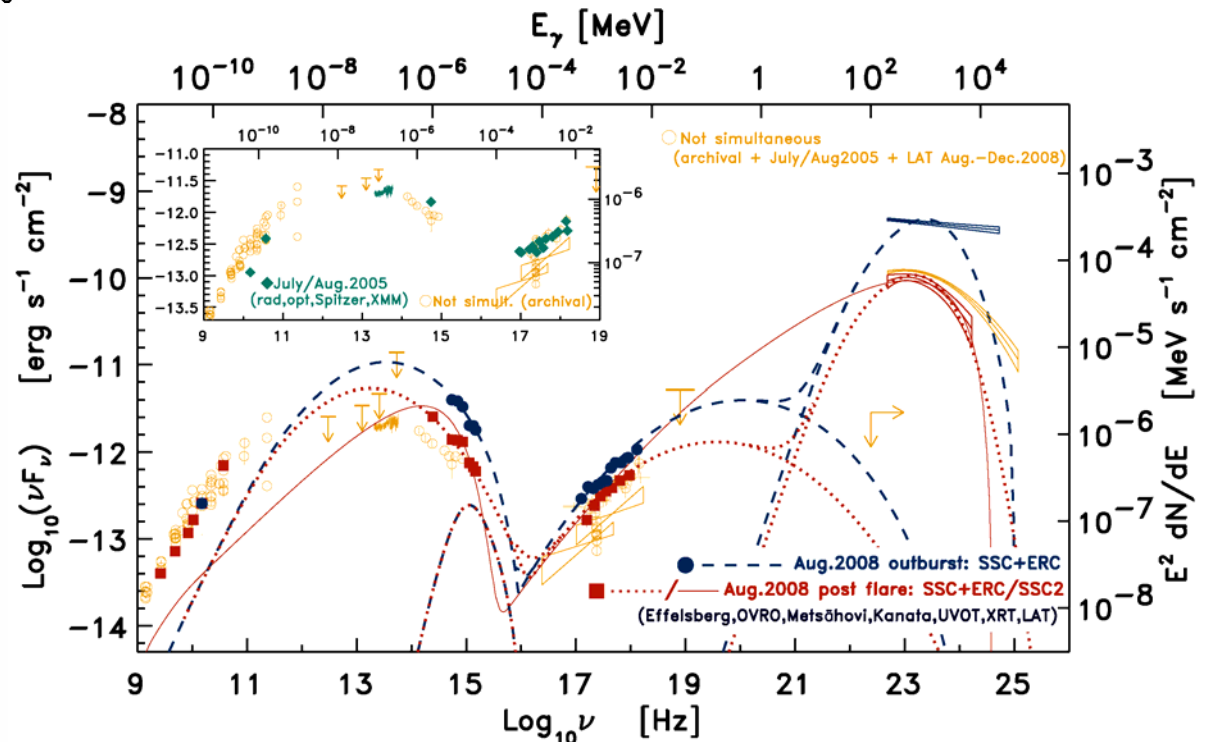
Variable multifrequency SED

The radio-to-gamma-ray averaged SEDs collected during the *Fermi-Swift* Aug.2008 multi-frequency campaign for both the outburst state (MJD: 54685-54689, blue data points) and the subsequent post-flare state (MJD 54690-54701, red data points). The archival data (published and unpublished and analyzed in this paper) are reported on background (orange data points).

Stefano Ciprini

Conclusions: Gamma-ray MONO-BAND variability

❑ Gamma-ray variability timescales were observed ranging from fractions of a day to months.

❑ Lower activity states studied as well for the first time in GeV band. High states do not exceed 1/4 of the total range.

❑ FSRQs and LSP/ISP BL Lac objects showed largest variations.

❑ PKS 1510–08, PKS 1502+106, 3C 454.3, 3C 279, PKS 0454–234 (all FSRQs), and 3C 66A and AO 0235+164 were the most bright and violently variable gamma-ray blazars during the first 11-months of Fermi survey.

❑ PKS 1502+106 (OR 103), 4C 38.41 (S4 1633+38) and 3C 454.3 were also the most intrinsically gamma-ray powerful.

❑ Different autocorrelation patterns, central lag amplitudes, zero crossing times, temporal trends and power-law indices are shown by DACF and SF. Different timescales and variability modes (more flicker- or Brownian-dominated).

❑ SFs point out a $1/f^a$ trend with values mostly distributed between 1.1 and 1.6.

❑ AO 0235+164 and 3C 454.3 showed fully Brownian weekly light curves.

❑ The brightest 28 sources the average PDS is described by a power law ($1/f^a$) without any evidence for breaks with a= 1.4±0.1 for FSRQs and 1.7±0.3 for BL Lacs.

❑ The two brighter HSP (Mkn 421 and PKS 2155–304) have PDS slopes of order 1. 3C 279 (slope of 2.3 in the X-ray band and 1.7 in the optical) showed a gamma-ray slope (1.6±0.2) closer to the optical PDS.

❑ Local flare shape analysis: stable baseline with sporadic flares or strong activity with complex temporal features.

❑ Average durations of the fitted flares varied from about 10 days up to 100 days in the case of S4 0917+44.

❑ In the few cases of marked asymmetric profiles, fast injection of accelerated particles and a slower radiative cooling and/or escape from the active region can be considered. Blend of several episodes could provide symmetric flares.

❑ 2 "flavors" of variability: rather constant baseline with sporadic flaring activity showing also intermittence (flatter PDS slopes, more flickering), and a few sources with strong activity with complex and structured time profiles characterized by the long memory and steeper PDS slopes (typical of random-walk, more Brownian).

❑ Traveling traveling shock fronts, single or multiple emission regions, versus instabilities and turbulence in the accretion flow causing intermittence.

❑Our systematic investistation can also serve as preparatory study for more detailed analysis case by case.

❑ Various interband (radio, optical, X-ray, TeV) timing correlations have been observed in several gamma-ray blazars, probing the emitting particle/jet dynamics.

Only the case of PKS 1502+106 is reported in this presentation:

❑ With the discovery of gamma-ray emission from the distant blazar PKS 1502+106, Fermi LAT is showing well its nature of optimal companion of both intensive coordinated multifrequency campaigns and lower sampling but longer term multi-waveband monitoring of blazar variability from the ground.

❑ PKS 1502+106 was the target the first Fermi MW campaign not planned in advance (ToO campaing). Simultaneous Swift observation and cross correlated optical-UV-X-ray-gamma-ray variability allowed identification of this source.

❑ PKS 1502+105 is a new gamma-ray blazar discovered by Fermi (poorly known above radio-mm frequencies). It is a FSRQ. Sure identification by optimal localization and cross-correlated variability. A very powerful sub-Gev peaked gamma-ray emitter, very variable, BLR-ERC (but also SSC) emission important, possible flare precursor signature in VLBA.

❑ PKS 1502+106: interesting source for radio-gamma-ray connection studies, and spectral-temporal variability studies.

❑ Thanks to this source also the optimal synergy between Fermi and Swift was demonstrated.